European Journal of Mechanics / A Solids 72 (2018) 57–65

Contents lists available at ScienceDirect

European Journal of Mechanics / A Solids

journal homepage: www.elsevier.com/locate/ejmsol

Linear spring stiffnesses for two-dimensional finite element modeling of arteries

J.A. Baier-Saip[a,*], P.A. Baier[b], J.C. Oliveira[c], H. Baier[d]

[a] Universidad Católica del Maule, Facultad de Ciencias Básicas, Av. San Miguel 3605, Casilla 617, Talca, Chile
[b] Instituto Federal de Educação, Ciência e Tecnologia do Ceará, Rua Estevão Remígio 1145, Limoeiro do Norte, CE, Brazil
[c] Laboratório Nacional de Computação Científica, Av. Getúlio Vargas 333, Petrópolis, RJ, Brazil
[d] Universität Würzburg, am Hubland, 97074 Würzburg, Germany

ARTICLE INFO

Keywords:
Elasticity tensor
Normal and angular springs
Stiffnesses

ABSTRACT

The physical properties of arteries are important in the research of the circulatory system dynamics. Moreover, in order to build Virtual Reality Simulators, it is crucial to have a tissue model able to respond in real time. A reduced mesh size results in shorter processing times, which can be achieved using a two-dimensional grid. In this work, a triangular topology is considered and the nodes are connected by three kinds of linear springs (one normal and two angular ones). The spring stiffnesses depend on the mesh geometry and on the elastic properties of the artery. The model linearizes the material response, but it still contemplates the geometric nonlinearities. Comparisons showed a good match with a nonlinear model and with our previous model based on a quadrilateral topology. However, the proposed model extension is more flexible and easier to implement than the previous one.

1. Introduction

Conducting clinical research is expensive, time-consuming, and manipulating biological variables is very challenging (Gwak et al., 2010). Although mathematical modeling may be difficult in some cases, virtual cardiovascular simulations are inexpensive and variables can be easily controlled (Zannoli et al., 2009). For example, studies of atherosclerotic plaques have evaluated the 3D stress distributions within plaques under certain loading and boundary conditions, so to analyze the biomechanical response to geometrical, structural, and material changes (Creane et al., 2010; Cilla et al., 2012; Morlacchi et al., 2013; Holzapfel et al., 2014).

A better understanding of the arterial wall mechanics can provide relevant information for medical diagnosis and therapies of some vascular pathologies (Garcia-Herrera et al., 2012). Indeed, the measurements of the arterial tree stiffness can be applied in routine clinical practice for risk stratification (Pereira et al., 2015). Detailed knowledge of vascular tissue properties is required to improve procedures such as angioplasty, to design arterial prostheses, and to describe the dynamics of the interaction between the heart and the circulatory system (Holzapfel et al., 2002). Moreover, physiological and pathological changes in the cardiovascular system directly influence the mechanical behavior of arterial walls (Diez, 2007).

The arterial wall is incompressible, anisotropic, inhomogeneous, highly nonlinear, and exhibits hysteresis under a cyclic load (Holzapfel and Ogden, 2010; Li, 2016). Usually, only the passive behavior of the tissue is considered, but even so, a complex set of equations results and a considerable amount of processing time is used to obtain the solution.

In order to show the artery deformations caused by the introduction of medical devices, a truthful Virtual Reality Simulator(VRS) must consider the physical models of the device and of the artery (Alderliesten et al., 2007; Wang et al., 2014; Baier et al., 2015, 2016). Due to its strong mathematical background, Finite Element Methods (FEM) are physically accurate (Garcia et al., 2006) and linear FEM are the most popular technique to model tissue deformation in VRS (Misra et al., 2008). The FEM have shown to be robust for the quantification of arterial stresses, and they have been successfully utilized for modeling of the stent-artery interaction. Balloon expandable stents have also been compared with self-expanding stents in terms of the level of stresses they induce within the arterial wall, and hence the risk of arterial injury.

A VRS must work in real time. For example, a haptic device demands a minimum refresh rate of 500 Hz, so that the user can experience a continuous (smooth) contact feeling. Thus, the reaction force due to tissue deformations has to be calculated very quickly. Although commercially available finite element codes take into account several

* Corresponding author.
E-mail address: jbaier@ucm.cl (J.A. Baier-Saip).

https://doi.org/10.1016/j.euromechsol.2018.04.013
Received 5 January 2018; Received in revised form 13 March 2018; Accepted 13 April 2018
Available online 21 April 2018
0997-7538/

physical aspects of arteries (including nonlinearities), the computation time would be too long for VRS. The model developed in this paper is intended to be used in fast calculations of artery deformations, where an exact response is not necessary.

In particular, the artery deformations produced by a catheter wire are tiny, and in this case the linear approximation is adequate. Hence, linearizations are adopted in the calculations of the elasticity tensor and of the spring stiffnesses. Furthermore, the method is based on a structural mechanic approach, because a VRS only requires the force feedback at the contact points and not the knowledge e.g. of a stress field at the surface.

A two-dimensional mesh is proposed and so the numerical difficulties arising from the isochoric constrain in three dimensions are avoided. This paper is organized as follows, in Section 2 the stiffness tensor component $C_{\eta\eta\eta\eta\mathbf{t}}$ is estimated, from which $C_{\theta z\theta z\mathbf{t}}$ can be calculated. Furthermore, the interaction between the nodes is simulated using normal, angular in plane, and angular out of plane springs. Then, in Section 3 the stiffnesses are determined and the results are analyzed.

2. Methods

When accuracy is not the most relevant aspect, a reduced mesh size and a linearization increase the computing performance. The model developed in this work is equivalent to a linear FEM using a triangular mesh with few nodes. First, additional stiffness tensor components are estimated and, afterwards, the formulas for calculating the stiffness of the springs are deduced.

2.1. Stiffness tensor

Fiber dispersion in collagenous soft tissues has an important influence on the mechanical response (Holzapfel and Ogdeon, 2017). There exist two different approaches for modeling fiber dispersion: the “angular integration” (Lanir, 1983) and the “generalized structure tensor” (Gasser et al., 2006). Both models have equivalent predictive power, and from the theoretical point of view neither of these models is superior to the other. However, the generalized structure tensor has proved to be very successful in modeling the data from experiments on a wide range of tissues. Furthermore, it is easier to analyze, simpler to implement, and the related computational effort is much lower than the angular integration approach.

Holzapfel et al. (2015) provide an overview of the main existing continuum nonlinear mechanical models of arteries, which have proven to give reliable results. In general, classical continuum mechanics assumes that the constitutive models and the corresponding simulations start from an unloaded, stress-free reference configuration (Pierce et al., 2015). This has been used to calculate the amount of stress applied to the tissue and its associated strain response (Fung, 1993; Humphrey, 2002; Vito and Dixon, 2003; Sokolis, 2008).

However, the boundary value problem of interest represents a loaded geometry and includes residual stresses. It has been shown that residual stresses make the stress distribution more homogeneous within each arterial layer (Fung, 1991). The modeling of residual deformations take into account the stress and bending, which are axially dependent. In order to take into account the residual stretches in our model, it would be necessary to calculate in a previous step the stresses and prestresses using a continuum mechanics approach (Pierce et al., 2015). Then the resulting stretches can be used to compute the inhomogeneous stiffness tensor (see below), which in turn is used to compute volume averages (Section 2.2). Nevertheless, this will not be pursued mainly because in our model only a two-dimensional picture is obtained, and the stress variation within a layer cannot be observed.

Usually, only planar biaxial deformations (tangential stretch λ_θ and axial stretch λ_z) are performed in experiments to obtain the most relevant information about the material properties. Nonetheless, this is not sufficient to characterize all material properties of soft tissues (Holzapfel and Ogden, 2009). In the present work, the energy density function for the arterial layer $\mathbf{t}$ (Intima, Media, or Adventitia) is given by

$$\Psi_{\mathbf{t}} = \mu_{\mathbf{t}}(I_1 - 3) + \frac{k_{1\mathbf{t}}}{k_{2\mathbf{t}}}(\Gamma_{\mathbf{t}} - 1)\,, \tag{1}$$

where

$$\Gamma_{\mathbf{t}} = e^{k_{2\mathbf{t}}[(1-\rho_{\mathbf{t}})(I_1-3)^2+\rho_{\mathbf{t}}(I_{4\mathbf{t}}-1)^2]}\,. \tag{2}$$

Further, the invariants I_1, $I_{4\mathbf{t}}$ are defined by

$$I_1 = \lambda_\theta^2 + \lambda_z^2 + \frac{1}{\lambda_\theta^2\lambda_z^2}\,,$$

$$I_{4\mathbf{t}} = \lambda_\theta^2\cos^2\phi_{\mathbf{t}} + \lambda_z^2\sin^2\phi_{\mathbf{t}}\,, \tag{3}$$

and the physical parameters of the layers $\mu_{\mathbf{t}}$, $k_{1\mathbf{t}}$, $k_{2\mathbf{t}}$, $\rho_{\mathbf{t}}$, $\phi_{\mathbf{t}}$ were experimentally obtained from the coronaries of human cadavers (Holzapfel et al., 2005). In particular, the energy density invariants capture structural aspects of the tissue (e.g. the orientation and dispersion of collagen fibers).

The stiffness tensor components $C_{\theta\theta\theta\theta\mathbf{t}}$, $C_{zzzz\mathbf{t}}$, and $C_{\theta\theta zz\mathbf{t}}$ of layer $\mathbf{t}$ were determined in Ref. (Baier-Saip et al., 2017). However, the calculations of the angular spring stiffnesses (Section 2.2) require also the knowledge of the tensor component $C_{\eta\eta\eta\eta\mathbf{t}}$. In order to find $C_{\eta\eta\eta\eta\mathbf{t}}$, it is necessary to write the stretches λ_θ and λ_z appearing in the energy density in terms of $\lambda_\parallel$ (the stretch parallel to the vector $\mathbf{e}_\parallel$, see Fig. 1). To this end, consider the point A_0 with coordinate (1,1). If the body is subjected to an initial deformation specified by the stretches $\lambda_{\theta 0}$ and λ_{z0}, the new coordinate will be $(\lambda_{\theta 0}, \lambda_{z0})$ (point A_1). After displacing this point a distance δ in the direction of $\mathbf{e}_\parallel$, the coordinate becomes $(\lambda_{\theta 0} + \delta\cos\eta, \lambda_{z0} + \delta\sin\eta)$ (point A_2). The stretch ratio equals the final length divided by the initial length parallel to the axis, which is equal to 1

$$\lambda_\theta = \lambda_{\theta 0} + \delta\cos\eta\,,$$

$$\lambda_z = \lambda_{z0} + \delta\sin\eta\,.$$

Moreover, the projections of the segments $\overline{OA_0}$ and $\overline{OA_2}$ along the vector $\mathbf{e}_\parallel$, are $\cos\eta + \sin\eta$ and $\lambda_{\theta 0}\cos\eta + \lambda_{z0}\sin\eta + \delta$ respectively. Thus, the stretch ratio is

$$\lambda_\parallel = \frac{\lambda_{\theta 0}\cos\eta + \lambda_{z0}\sin\eta + \delta}{\cos\eta + \sin\eta} = \frac{\lambda_\theta\cos\eta + \lambda_z\sin\eta}{\cos\eta + \sin\eta}\,. \tag{4a}$$

The projections of the segments $\overline{OA_0}$ and $\overline{OA_2}$ along the vector $\mathbf{e}_\perp = -\sin\eta\mathbf{e}_\theta + \cos\eta\mathbf{e}_z$ perpendicular to $\mathbf{e}_\parallel$, are $\cos\eta - \sin\eta$ and

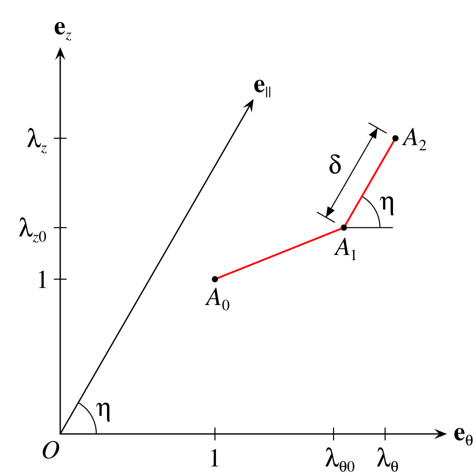

Fig. 1. Coordinates of a point in a body without stretch (point A_0), with an initial stretch (point A_1), and after an additional deformation parallel to $\mathbf{e}_\parallel$ (point A_2). The unit vector $\mathbf{e}_\parallel$ is in the plane of $\mathbf{e}_\theta$ and $\mathbf{e}_z$. Besides, the angle between $\mathbf{e}_\parallel$ and $\mathbf{e}_\theta$ is η.